Electronic Supplementary Material (ESI) for Dalton Transactions.

Supplementary Information for

J. Malina, P. Scott, V. Brabec: Recognition of DNA/RNA bulges by antimicrobial and antitumor metallohelices

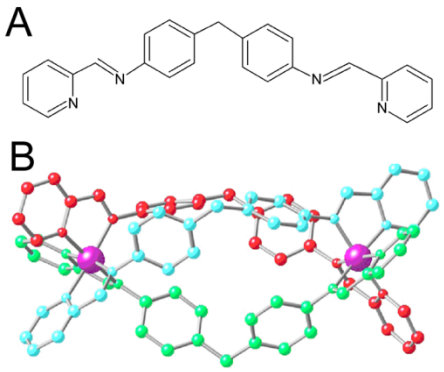

Figure S1. (A) Structure of **I** (**I** = $C_{25}H_{20}N_4$) and (B) 3D structure of *M*-$[Fe_2(\mathbf{I})_3]^{4+}$.

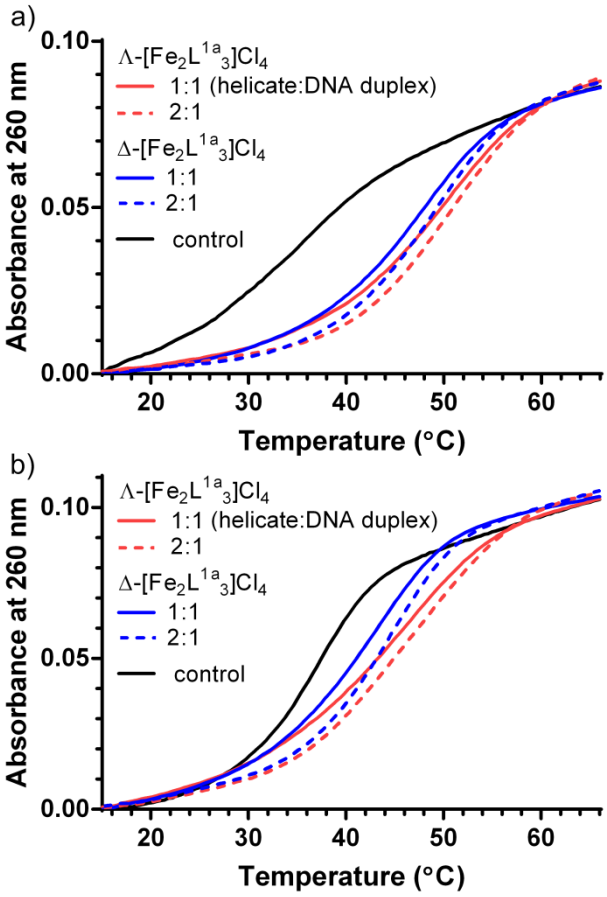

Figure S2. Melting curves for G-*C2*-G (a) and C-*A2*-C (b) DNA bulges in the presence of Λ- and Δ-$[Fe_2\mathbf{L^{1a}}_3]Cl_4$.

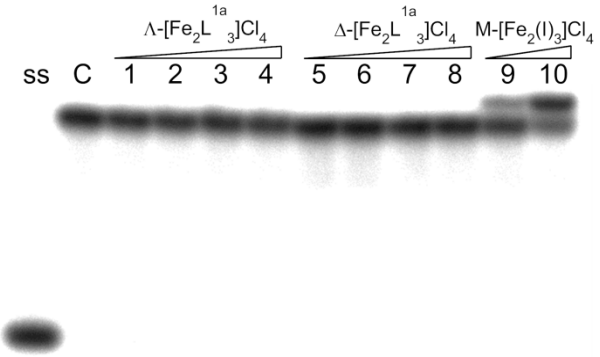

Figure S3. Autoradiogram of the gel run at 5 ˚C, demonstrating interactions of the flexicates with the T-*A3*-T(14) bulge. Lane ss: control containing one strand in the buffer. Lane C: control containing duplex in the buffer in the absence of the flexicates. Lanes 1-4: duplex mixed with Λ-[Fe_2**L**$^{\mathbf{1a}}{}_3$]Cl_4 at 0.5:1, 1:1, 1.5:1 and 2:1 (flexicate:duplex) ratios, respectively. Lanes 5-8: duplex mixed with Δ-[Fe_2**L**$^{\mathbf{1a}}{}_3$]Cl_4 at 0.5:1, 1:1, 1.5:1 and 2:1 (flexicate:duplex) ratios, respectively. Lanes 9, 10: duplex mixed with the *M*-[Fe_2(**I**)$_3$]Cl_4 at 0.5:1 and 1:1 (helicate:duplex) ratios, respectively.

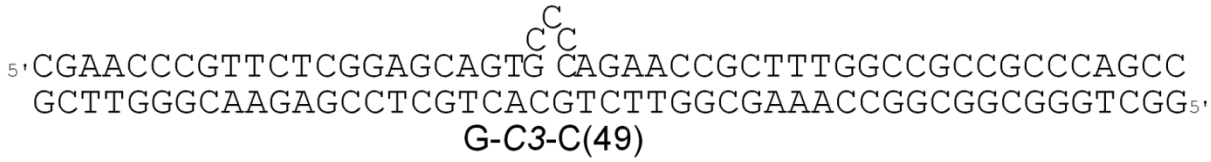

Figure S4. Sequence of the 49-bp long duplex containing a single three-cytosine bulge flanked by guanine and cytosine on the 5'-side and 3'-side, respectively used in the present study and its abbreviation.

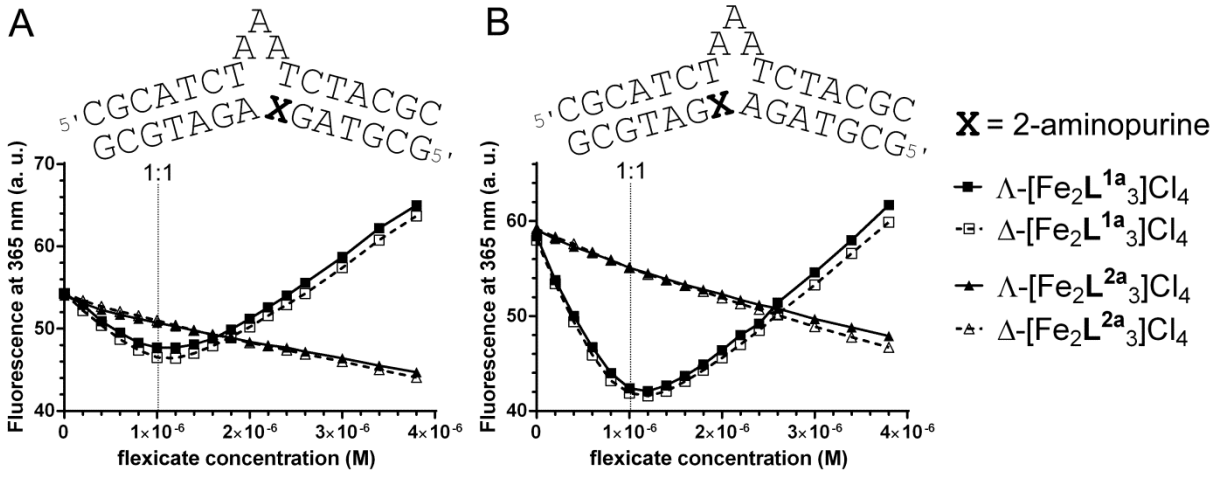

Figure S5. Fluorescence titrations of the T-*A3*-T(14) bulged duplex (1 μM) labelled by 2AP in the sequence opposite the bulge with the enantiomers of [Fe_2**L**$^{\mathbf{1a}}{}_3$]Cl_4 and [Fe_2**L**$^{\mathbf{2a}}{}_3$]Cl_4 flexicates. The buffer conditions were 10 mM sodium phosphate buffer (pH 7) and 100 mM NaCl.

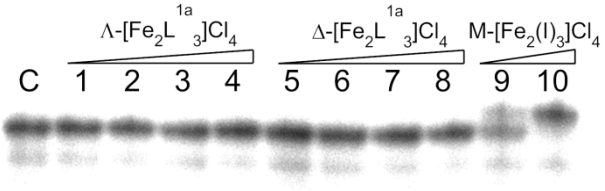

Figure S6. Autoradiogram of the gel run at 5 ˚C. Lane C: control containing the TAR RNA in the buffer in the absence of the flexicates. Lanes 1-4: TAR RNA mixed with Λ-$[Fe_2\mathbf{L^{1a}}_3]Cl_4$ at 0.5:1, 1:1, 1.5:1 and 2:1 (flexicate:TAR RNA) ratios, respectively. Lanes 5-8: TAR RNA mixed with Δ-$[Fe_2\mathbf{L^{1a}}_3]Cl_4$ at 0.5:1, 1:1, 1.5:1 and 2:1 (flexicate:TAR RNA) ratios, respectively. Lanes 9, 10: TAR RNA mixed with the *M*-$[Fe_2(\mathbf{I})_3]Cl_4$ at 0.5:1 and 1:1 (flexicate:TAR RNA) ratios, respectively.

The sample of control TAR RNA yielded an extra faint band migrating slightly faster than the major strong band. The presumed cause of this observation is a lower stability of RNA (in comparison with DNA). RNA decomposes relatively rapidly and had to be prepared for each experiment fresh by its isolation from the polyacrylamide gel. It implies that the second band in the Figure S6 very likely corresponds to degraded TAR RNA from which one nucleotide on the 3' side was cut off. Nevertheless, the results indicate that the flexicates do not bind TAR RNA strongly enough to ensure intactness of the resulting complex during its migration in the gel.